

# Architecture and characterization of sarcosine oxidase from *Thermococcus kodakarensis* KOD1

Sangmin Lee · Baolei Jia · Bang Phuong Pham ·  
Yongqi Shao · Jae Myeong Kwak · Gang-Won Cheong

Received: 8 August 2011 / Accepted: 20 October 2011 / Published online: 15 November 2011  
© Springer 2011

**Abstract** Sarcosine oxidase (SOX) catalyzes the oxidation of the methyl group in sarcosine and transfer of the oxidized methyl group into the one-carbon metabolic pool. Here, we separately cloned and expressed  $\alpha$  and  $\beta$  subunit of SOX from *Thermococcus kodakarensis* KOD1 (TkSOX) in *Escherichia coli* and the recombinant proteins were purified to homogeneity. Gel filtration chromatography and transmission electron microscopy analysis showed that the  $\alpha$  subunit formed a dimeric structure and behaved as an NADH dehydrogenase;  $\beta$  subunit was a tetramer that had sarcosine oxidase and L-proline dehydrogenase activity. The TkSOX complex assembled into the hetero-octameric  $(\alpha\beta)_4$  form and had NADH dehydrogenase activity. Gold-label analysis indicated that  $\alpha$  and  $\beta$  subunits were oriented in the alternative form. Based on these results, we

suggested that TkSOX was a multifunctional enzyme and that each subunit and  $(\alpha\beta)_4$  complex may separately exist as a function enzyme in different conditions.

**Keywords** Sarcosine oxidase · *Thermococcus kodakarensis* KOD1 · Electron microscopy

## Abbreviations

SOX Sarcosine oxidase  
IPTG Isopropyl- $\beta$ -D-1-thiogalactopyranoside  
EM Electron microscopy

## Introduction

Sarcosine is a common soil metabolite of creatinine, which animals excrete in urine, and various soil bacteria can utilize sarcosine as a nitrogen and carbon source. Sarcosine oxidase (SOX, EC 1.5.3.1) is an enzyme that catalyzes the oxidation of the methyl group in sarcosine to yield equimolar glycine, hydrogen peroxide, and formaldehyde or 5, 10-methylenetetrahydrofolate. Many organisms have been found to produce intracellular SOX, such as bacteria (Suzuki 1981; Nishiya and Imanaka 1993; Meškys et al. 1996; Hassan-Abdallah et al. 2005), mammals (Chikayama et al. 2000), and plant (Goyer et al. 2004). SOX with creatininase and creatinase have been used in clinics for the determination of creatinine, which is an important parameter to estimate the function of kidney (Nagata et al. 2005). For clinical applications of enzymes, thermostability is an essential property that has advantages in transportation, storage, and clinical application.

In different organisms, SOXs exist with different subunit composition (monomer, hetero-dimer, hetero-tetramer,

Communicated by H. Atomi.

S. Lee, B. Jia, B.P. Pham, and Y. Shao contributed equally to the study.

**Electronic supplementary material** The online version of this article (doi:10.1007/s00792-011-0408-x) contains supplementary material, which is available to authorized users.

S. Lee · B. Jia · B. P. Pham · Y. Shao · J. M. Kwak ·  
G.-W. Cheong (✉)  
Division of Applied Life Sciences (BK21 Program),  
Gyeongsang National University, Jinju 660-701, Korea  
e-mail: gwcheong@gnu.ac.kr

B. Jia  
College of Plant Sciences, Jilin University,  
Changchun 130-062, China

G.-W. Cheong  
Environmental Biotechnology National Core Research Center,  
Gyeongsang National University, Jinju 660-701, Korea

and hetero-octamer). Monomeric SOX is a prototypical member of a recently recognized family of amine-oxidizing enzymes in both eukaryotes and prokaryotes, all of which contain covalently bound flavin (Willie and Jorns 1995; Wagner and Schuman Jorns 1997). Hetero-dimeric SOX from *Alcaligenes denitrificans* is composed of two different subunits (Kim et al. 1987). Hetero-tetrameric SOX is an enzyme with a molecular mass of ~180 kDa, which contains four subunits ( $\alpha$ ,  $\beta$ ,  $\gamma$ ,  $\delta$ ), three coenzymes (NAD, FMN, FAD), a zinc ion and a binding site for hydrofolate. In *Pyrococcus horikoshii* OT3, PH1363 and PH1364, a hetero-octameric complex ( $\alpha\beta$ )<sub>4</sub>, are annotated as sarcosine oxidase in the genome sequence because of their high homology with a monomeric SOX. But neither of these enzymes exhibits any sarcosine oxidase activity. In contrast, the proteins show high L-proline dehydrogenase activity (Kawakami et al. 2005).

In the present study, we separately purified the  $\alpha$  and  $\beta$  subunits of SOX from *Thermococcus kodakarensis* KOD1 (TkSOX). Using transmission electron microscopy (TEM) and gel filtration chromatography, we revealed that the  $\alpha$  subunit displayed dimeric or tetrameric forms. While the  $\alpha$  subunit had NADH dehydrogenase activity, the  $\beta$  subunit, a tetrameric structure, had both sarcosine oxidase and L-proline dehydrogenase activity. Finally, TEM analysis indicated that TkSOX forms a hetero-octameric ( $\alpha\beta$ )<sub>4</sub> complex, which showed NADH dehydrogenase activity.

## Materials and methods

### Microorganisms and media

*T. kodakarensis* KOD1 (with accession number:12380 in Japan Collection of Microorganisms), kindly donated by JCM, RIKEN BioResource Center, Japan, was used to prepare crude cell extracts and isolated genomic DNA. It was cultured in the 280 *Thermococcus* medium under anaerobic conditions at 85°C (Fukui et al. 2005).

### Cloning and expression of $\alpha$ and $\beta$ subunit of TkSOX

*TK0116* and *TK0117* genes, encoding the  $\alpha$  and  $\beta$  subunits of TkSOX, respectively, were amplified from *T. kodakarensis* KOD1 genomic DNA (Fukui et al. 2005) by PCR and cloned into pET28(a) vector (Novagen). The primers for *TK0116* (5'-CAT ATG AGA CCG CTT GAC CTA AC and 5'-CTC GAG TCA ATC CCT CCC CGC GAC GA) and *TK0117* (5'-CAT ATG CCG ACG AGA GAG CTT C and 5'-CTC GAG TCA CCC CAT CTG CAG GGC CT) were designed based on *T. kodakarensis* KOD1 genomic sequence. The resulting DNA constructs were used for protein expression. The expression of  $\alpha$  and  $\beta$  subunits was induced in

*Escherichia coli* BL21(DE3) (Novagen) by the addition of 1 mM of isopropyl- $\beta$ -D-1-thiogalactopyranoside (IPTG). The cells were harvested and resuspended in lysis buffer (50 mM NaH<sub>2</sub>PO<sub>4</sub>, 300 mM NaCl and 10 mM imidazole, pH 8.0). After disruption of cells by sonication, total proteins were loaded onto nickel-NTA resins (Bio-Rad) pre-equilibrated with lysis buffer. The  $\alpha$  and  $\beta$  subunits were eluted with around 250 mM imidazole. Purified  $\alpha$  and  $\beta$  subunits were examined by SDS polyacrylamide gel electrophoresis (PAGE) according to the standard procedure (Hames 1998).

### Gel filtration chromatography

Gel filtration chromatography analysis of purified proteins or protein mixtures was performed using a Superdex 200 10/30 column (GE Healthcare) on an FPLC system (Bio-Rad). Protein standards included thyroglobulin (669 kDa), ferritin (440 kDa), catalase (232 kDa), aldolase (158 kDa), albumin (67 kDa), and ovalbumin (43 kDa). The collected protein samples were examined by SDS-PAGE and native-PAGE.

### Nanogold cluster localization

To identify the position of each subunit in the SOX complex, we used nanogold cluster localization method. Firstly, 100  $\mu$ g of purified  $\alpha$  and  $\beta$  subunits was incubated with thrombin for 16 h at 22°C to cleave the 6\*His-tag in the PBS buffer (140 mM NaCl, 2.7 mM KCl, 10 mM Na<sub>2</sub>HPO<sub>4</sub>, 1.8 mM KH<sub>2</sub>PO<sub>4</sub>, pH 7.3). The reaction mixture was heated at 80°C for 20 min to inactivate thrombin and loaded on nickel-NTA resins. The non-tag proteins were eluted by PBS buffer and only used to determine the position of each subunit. 6\*His  $\alpha$  subunit was mixed with non-tag  $\beta$  subunit to produce the complex; then the produced homogenous complex protein particles were incubated with Nanogold probe at room temperature for 10 min and applied to TEM. Similarly, 6\*His- $\beta$  subunits were mixed with non-tag  $\alpha$  subunits and the oligomerized complex was incubated with nanogold and checked by TEM.

### Electron microscopy and image processing

$\alpha$ ,  $\beta$ , and ( $\alpha\beta$ )<sub>4</sub> complex were applied to glow-discharged carbon-coated copper grids. Allowing the protein to adsorb for 3 min, the grids were rinsed with deionized water and stained with 2% (w/v) uranyl acetate. Specimens were examined in the FEI Technai-12 at an acceleration voltage of 120 kV using a low-dose unit. Electron micrographs (EM) were recorded on Kodak film (SO163) at a nominal magnification of 51,600 $\times$  or 67,000 $\times$ . For image processing, the SEMPER (Saxton et al. 1979) and EM software (Hegerl 1996) packages were used. The individual images were aligned translationally, but not rotationally (Baumeister et al. 1988; Marco et al. 1994; van Heel and Frank 1981).

## Enzyme activity assay

To measure the sarcosine oxidase activity, 0.1 ml of enzyme solution (0.5–30  $\mu$ g protein) was added into a 0.9 ml of 250 mM sodium pyrophosphate buffer, pH 8.0, containing 0.1 M sarcosine as substrate (Guo et al. 2006). After 10 min of incubation at 80°C, the reaction was terminated with 0.25 ml of 1 M acetic acid. The formaldehyde formed in this reaction was measured by the method of Nash (Brunker et al. 1997).

Dye-linked L-proline dehydrogenase activity (dye-L-proDH) was assayed by measuring the reduction rate of 2,6-dichloroindophenol (DCIP) as previously described (Sakuraba et al. 2001). The standard reaction mixture was composed of 100 mM L-proline, 0.1 mM DCIP, 200 mM Tris-HCl buffer (pH 8.0), and 0.5–30  $\mu$ g proteins in a total volume of 1.0 ml. The mixture without the substrate (L-proline) was previously incubated at 80°C for about 3 min in a cuvette with a 0.4-cm light path length and then the reaction was started by the addition of L-proline. The initial decrease in absorbance at 600 nm was measured with a recording spectrophotometer.

Dye-linked NADH dehydrogenase activity was assayed by measuring the decrease of DCIP at 600 nm in the presence of NADH. The reaction mixture was the same as that for the dye-L-proDH activity, except that L-proline was altered by NADH (0.1 mM) and FAD (0.05 mM) was added. The nonenzymatic decrease in DCIP in the presence of NADH at 80°C was monitored in the absence of enzyme.

## Results

### Amino acid sequence alignment of $\alpha$ and $\beta$ subunits

Sequence analysis by BLAST and Clustal W showed that the amino acid sequence of the  $\alpha$  and  $\beta$  subunits of TkSOX shared a significant level of identity with previously characterized dye-linked L-proline dehydrogenase from *Thermococcus profundus* (TpPDH), PDH1 and PDH2 from *P. horikoshii* OT-3 (PhPDH1 and PhPDH2) (Kawakami et al. 2004). The amino acids sequence of the TkSOX  $\alpha$  subunit exhibited 71, 31, and 34% homology to phPDH1 $\alpha$ , PhPDH2 $\alpha$ , and TpPDH $\alpha$ , respectively (Supplementary Fig. S1). The  $\beta$  subunit of TkSOX showed 88, 55, and 63% identities with that of PhPDH1 $\beta$ , PhPDH2 $\beta$ , and TpPDH $\beta$ , respectively (Supplementary Fig. S2). The previous reports revealed that both PhPDH2 and TpPDH had a native molecular mass of 120 kDa and formed an unusual  $\alpha\beta\gamma\delta$  hetero-tetrameric complex. Functional analysis of TpPDH revealed that the  $\beta$  subunit catalyzed the dye-linked L-proline dehydrogenase reaction and the  $\alpha$  subunit

exhibited dye-linked NADH dehydrogenase activity (Kawakami et al. 2005). Furthermore, PhPDH1, which is composed of  $\alpha$  and  $\beta$  subunits with 56 and 43 kDa, shows high similarity with TkSOX in both subunit composition and amino acid sequences. Biochemical analyses of each subunit revealed that PhPDH1 did not show any sarcosine dehydrogenase activity, the  $\beta$  subunit exhibited proline dehydrogenase activity, and the  $\alpha$  subunit possessed neither proline dehydrogenase nor NADH dehydrogenase activity (Kawakami et al. 2005; Tsuge et al. 2005).

### Structure of the $\alpha$ and $\beta$ subunits

To determine the oligomeric nature of TkSOX, we purified each subunit from recombinant *E. coli*. SDS-PAGE analysis revealed that the molecular masses of  $\alpha$  and  $\beta$  subunits were approximately 54 and 43 kDa, which were close to those of deduced amounts from amino acids sequences (Fig. 1). However, native-PAGE analysis under nondenaturing conditions showed two bands: the strong band represented a molecular weight approximately of 100 kDa corresponding to the size of a dimer of 54 kDa; the weak band represented molecular weight approximately of 200 kDa, corresponding to the size of a tetramer (Fig. 1Ab). To clarify the oligomeric structure, we performed electron microscopy using purified  $\alpha$  subunit. The electron micrographs of the negatively stained  $\alpha$  subunit showed two forms: dumbbell-shaped and ring-shaped structures (Fig. 1Ac). The amount ratio of dimer to tetramer in EM graphs coincided with the native-PAGE result. To obtain further insight into the molecular architecture of this protein, we performed image processing analysis by EM software package. The dumbbell-shaped and ring-shaped forms were separately selected and subjected to rotational and translational alignment and classified into different classes based on eigenvector data. The average of 235 dumbbell-shaped forms revealed a 2-fold symmetry with broad, high accumulation near the ends and tapering toward the middle. The average of 258 ring-shaped forms showed a structure with heavy stain accumulation in its center (Fig. 1Ac). In addition, the dimensions of the dimer or tetramer were 1  $\times$  6 nm (height and width) or 3  $\times$  6 nm (diameter of ring and central hole), respectively.

The purified  $\beta$  subunit was also analyzed by native-PAGE and EM. Native-PAGE showed single band with a molecular mass approximately of 160 kDa, indicating that the  $\beta$  subunit existed as a tetramer (Fig. 1Bb). The tetrameric structure was confirmed by EM and image processing analysis (Fig. 1Bc). Compared with the  $\alpha$  subunit, the electron micrographs of the negatively stained  $\beta$  subunit showed a uniform distribution of the ring-shaped structure in the top-view orientation. The average image of 235 revealed a 4-fold symmetric structure with heavy stain

**Fig. 1** Structural analysis of purified  $\alpha$  and  $\beta$  subunits of TkSOX. SDS-PAGE (Aa and Ba) and native-PAGE (Ab and Bb) analysis of TkSOX  $\alpha$  and  $\beta$  subunits. **c** Electron micrographs of  $\alpha$  and  $\beta$  subunits were obtained by negative staining with 2% uranyl acetate. The snapshot pictures show the average images. The *arrows* indicate the dimeric or tetrameric oligomer of the TkSOX  $\alpha$  subunit and tetrameric oligomer of the TkSOX  $\beta$  subunit

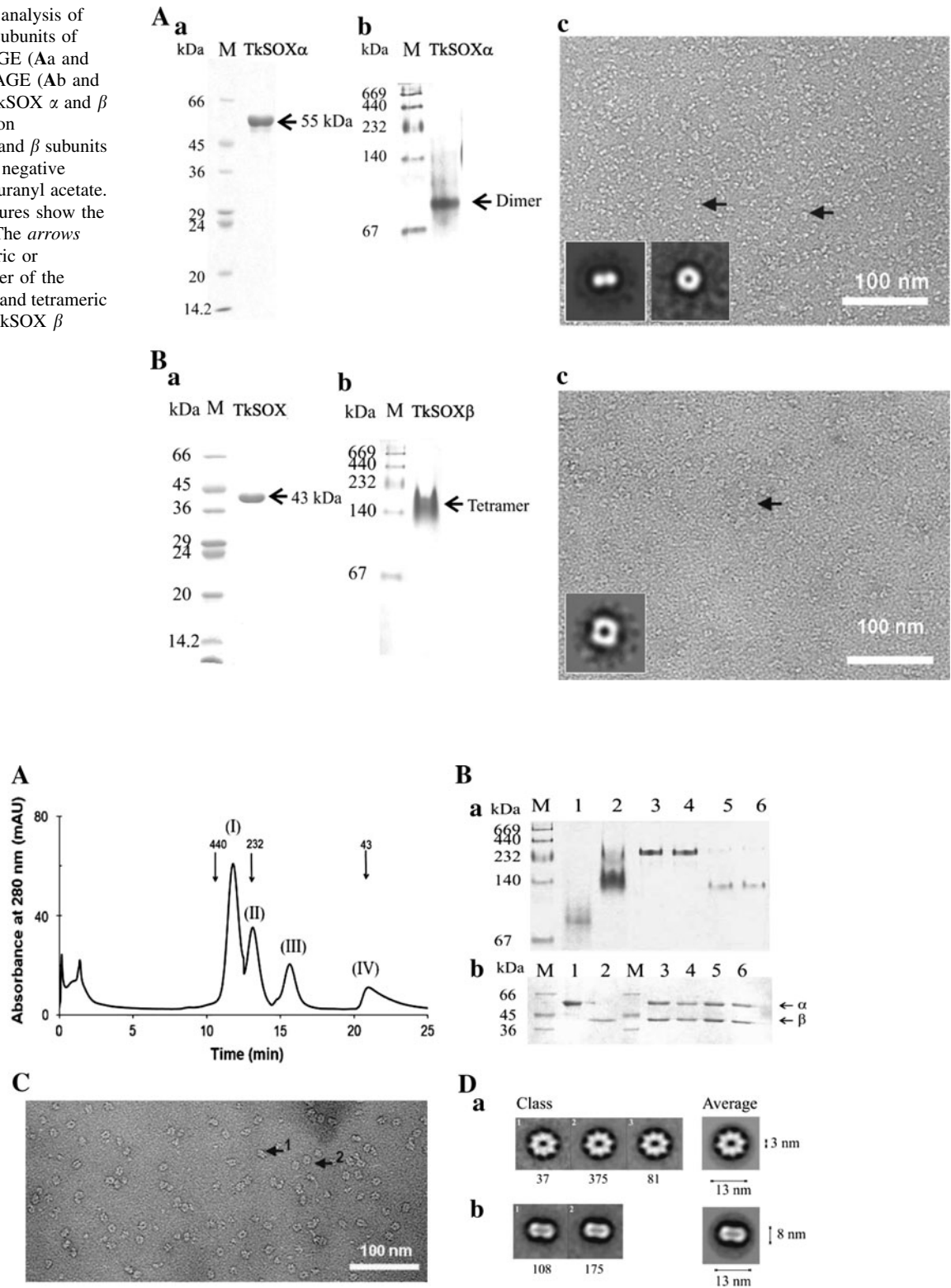


**Fig. 2** Structure of the hetero-octameric TkSOX ( $\alpha\beta$ )<sub>4</sub> complex. **A** TkSOX  $\alpha$  and  $\beta$  subunits were mixed and kept at room temperature for 1 h and loaded on a Superdex 200 10/300 GL column. The separated proteins were divided and pooled into four fractions: complex (I), intermediate (II),  $\alpha$  subunit (III) and  $\beta$  subunit (IV). **B** Proteins from gel filtration chromatography were subjected to SDS-

PAGE and native-PAGE. Lane M is the protein size marker; lane 1, lane 2, lanes 3–4, and lanes 5–6 correspond to fraction IV, III, I and II, respectively. **C** Electron micrograph was obtained by negative staining of the TkSOX complex with 2% uranyl acetate. Arrows indicate the top and side views of the TkSOX ( $\alpha\beta$ )<sub>4</sub> complex. **D** The image processing of the TkSOX ( $\alpha\beta$ )<sub>4</sub> complex

accumulation at its center (Fig. 1Bc). Its dimensions were a ring diameter of 8 nm and a central hole of 2 nm.

To determine the structure of the TkSOX complex, the  $\alpha$  and  $\beta$  subunits were mixed at room temperature for 1 h by 1:1 molecular ratio and the mixture was subjected to gel filtration chromatography. Four peaks (I, II, III, and IV) appeared in the curve (Fig. 2A). Including the peaks IV and III that were eluted at the same time with  $\alpha$  and  $\beta$  subunits alone, two new peaks, I and II, represented high molecular weight protein complex with molecular mass  $\sim 400$  and  $\sim 200$  kDa, respectively. SDS-PAGE analysis revealed that peaks I and II contained both  $\alpha$  and  $\beta$  subunits, but peaks IV and III only contained  $\alpha$  and  $\beta$  subunits, respectively. Furthermore, native-PAGE showed that the protein from peak I was a high molecular weight protein complex of about 400 kDa, while the protein from peak II showed two bands: the weak band was similar to the band from peak I and the strong band had a molecular mass of about 200 kDa (lanes 5 and 6 on Fig. 2Ba). The consistent results from gel filtration chromatography and native-PAGE analyses indicated that the peak I fractions were  $(\alpha\beta)_4$  complexes ( $\sim 400$  kDa), while peak II fractions were  $(\alpha\beta)_2$  complexes ( $\sim 200$  kDa), as the monomeric size of  $\alpha$  and  $\beta$  subunits was determined to be about 54 and 43 kDa. Interestingly, with the increasing incubation time at 4°C, the proteins in peak II could gradually convert to peak I (Supplementary Fig. S3), demonstrating that peak II was an intermediate state for the complex formation.

To further characterize the architecture of the TkSOX complex, peak I proteins were examined using negatively stained EM (Fig. 2C). The electron micrographs of the complex showed two basic views, top-on and side-on views, depending on the different orientations on the grid. A total of 493 top-on views of well-stained particles were translationally and rotationally aligned and classified into three groups, based on eigenvector-eigenvalue data analysis. The average image of top-on views revealed an 8-fold symmetry (Fig. 2Da). This result suggests that the complex behaves as a hetero-octamer consisting of four  $\alpha$  and four  $\beta$  subunits, which is consistent with the gel filtration analysis. A total of 283 side-on views showed a highly distorted doughnut form at the center region (Fig. 2Db). In addition, the diameters of the ring and the central hole were approximately 13 and 3 nm. The length and width of the side-on particle were 13 and 8 nm, respectively.

To clarify the arrangement of  $\alpha$  and  $\beta$  subunits in the complex, the nanogold labeling method was employed. The 6\*His-tag and non-tag proteins were prepared as described in ‘Materials and Methods’. The TkSOX complex formed by the 6\*His- $\alpha$  subunit and non-tag  $\beta$  subunit was labeled with gold that would bind the  $\alpha$  subunit only.

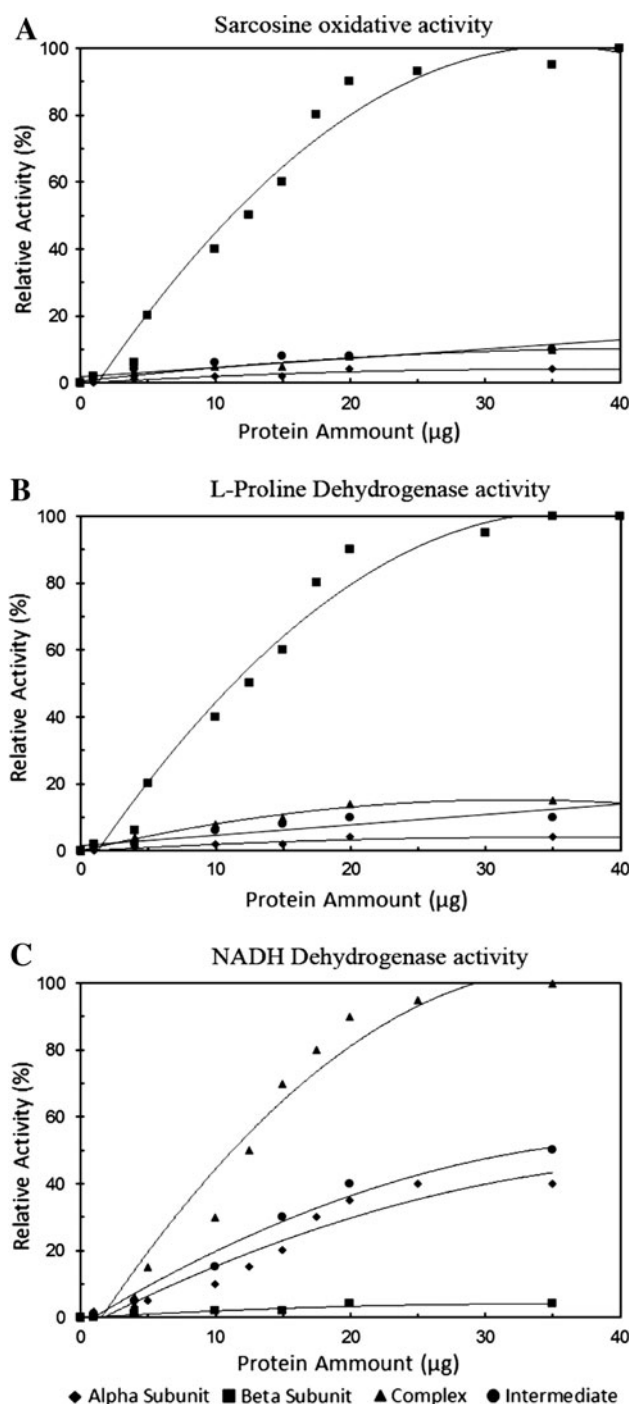


**Fig. 3** Activity analysis of TkSOX. Sarcosine oxidase activity of  $\alpha$  (filled diamonds),  $\beta$  (filled squares) subunit, intermediate (filled circles) and TkSOX (filled triangles) (a), L-proline dehydrogenase activity (b), and NADH dehydrogenase activity (c)

In contrast, TkSOX formed by the 6\*His- $\beta$  subunit and non-tag  $\alpha$  subunit was also labeled. Electron micrographs of the two kinds of labeled complexes revealed that the  $\alpha$  and  $\beta$  subunits in the  $(\alpha\beta)_4$  complex were localized in alternative forms (Supplementary Fig. S4).



### Activity assay of TkSOX

Based on sequence analysis, TkSOX may possess NADH dehydrogenase, L-proline dehydrogenase, and sarcosine oxidase activity. To characterize the functions of each subunit and complex, the three enzymatic assays were performed as described in “Materials and methods” (Fig. 3). Based on these results, we found that interestingly,  $\beta$  subunit displayed both sarcosine oxidase and L-proline dehydrogenase activity, but not NADH dehydrogenase activity. This result is different from a previous report, in that PhPDH1 could not detect any sarcosine oxidase activity. On the other hand, both the TkSOX complex and  $\alpha$  subunit showed NADH dehydrogenase activity, while the complex’s activity was higher than the  $\alpha$  subunit alone.

### Discussion

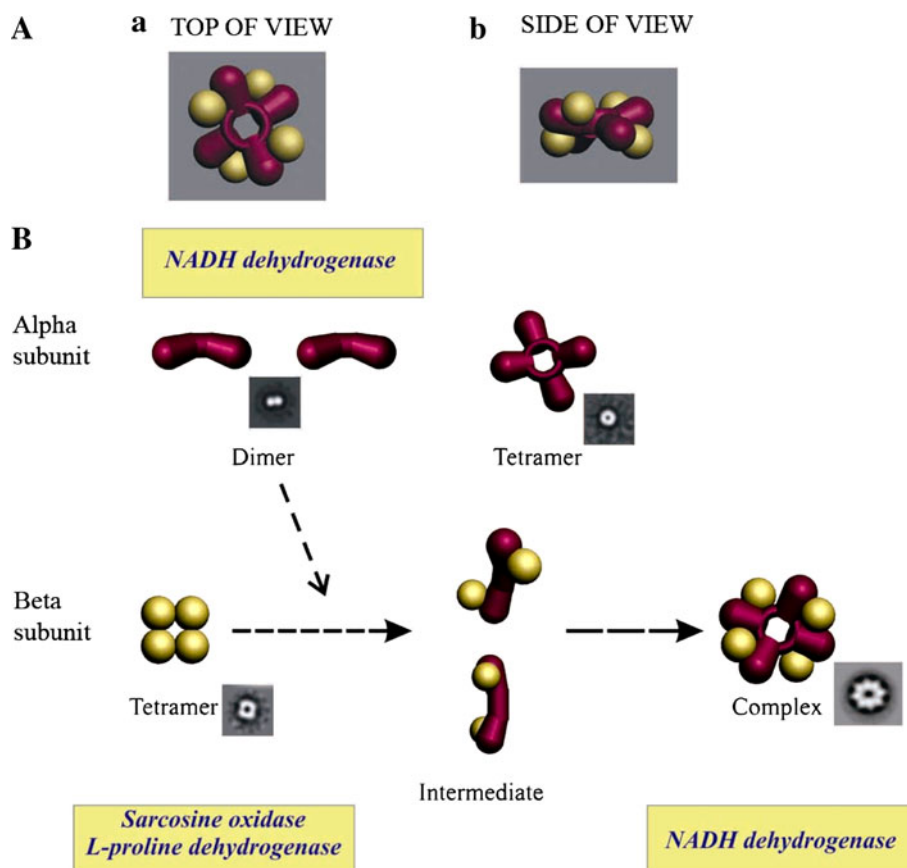
In this study, we described the architecture and function of TkSOX of hyperthermophilic origin, *T. kodakarensis* KOD1. Although the TkSOX gene is annotated as sarcosine oxidase in the *T. kodakarensis* KOD1 genome, due to its high homology with a monomeric sarcosine oxidase, this enzyme has multifunctional activities alone or as a

complex. Our results showed that TkSOX  $\alpha$  subunit had two kinds of particles: dimer and tetramer, and possessed NADH dehydrogenase activity. Its function was similar to the  $\alpha$  subunit of hetero-tetrameric sarcosine oxidase (Chen et al. 2006). The  $\beta$  subunit of TkSOX only showed one kind of homogeneous ring-shaped particle, which obviously had four mass centers. Activity assays indicated that the  $\beta$  subunit had both sarcosine oxidase and L-proline dehydrogenase activity, but no NADH dehydrogenase activity. This result revealed that the function of the  $\beta$  subunit was similar to most reported monomeric sarcosine oxidase (Suzuki 1994).

Here we also determined the assembly of TkSOX complex by gel filtration chromatography, native-PAGE, and EM. The results showed that the TkSOX complex consisted of four  $\alpha$  subunits and four  $\beta$  subunits, in the hetero-octameric form with molecular weight approximately 400. Using EM analysis and NTA–Nanogold probe, we showed that the  $\alpha$  and  $\beta$  subunits were localized alternately.

With these data, we proposed a model of SOX complex, its assembly process and the functional mechanism during the procedure (Fig. 4). When mixing the two subunits, the  $\alpha$  subunit, most of which were dimers and possessed NADH dehydrogenase activity, would bind to the ring-

**Fig. 4** A proposed assembly and functional mechanism of TkSOX based on structural analysis



shaped tetrameric  $\beta$  subunit to form the  $(\alpha\beta)_2$  intermediate. During this procedure, the sarcosine oxidase activity and L-proline dehydrogenase activity of the  $\beta$  subunit disappeared. Finally, the intermediate formed the hetero-octameric complex, which possessed higher NADH dehydrogenase activity than the dimeric  $\alpha$  subunit. Our study is the first reported description of architecture and function of a multi-functional archaeal SOX; however, the mechanisms of assembly and in vivo function will require further examination in future work.

## References

- Baumeister W, Dahlmann B, Hegerl R, Kopp F, Kuehn L, Pfeifer G (1988) Electron microscopy and image analysis of the multicatalytic proteinase. *FEBS Lett* 241:239–245
- Brunker P, Altenbuchner J, Kulbe KD, Mattes R (1997) Cloning, nucleotide sequence and expression of a mannitol dehydrogenase gene from *Pseudomonas fluorescens* DSM 50106 in *Escherichia coli*. *Biochim Biophys Acta* 1351:157–167
- Chen Z, Hassan-Abdullah A, Zhao G, Jorns MS, Mathews FS (2006) Heterotetrameric sarcosine oxidase: structure of a diflavin metalloenzyme at 1.85 Å resolution. *J Mol Biol* 360:1000–1018
- Chikayama M, Ohsumi M, Yokota S (2000) Enzyme cytochemical localization of sarcosine oxidase activity in the liver and kidney of several mammals. *Histochem Cell Biol* 113:489–495
- Fukui T, Atomi H, Kanai T, Matsumi R, Fujiwara S, Imanaka T (2005) Complete genome sequence of the hyperthermophilic archaeon *Thermococcus kodakarensis* KOD1 and comparison with *Pyrococcus* genomes. *Genome Res* 15:352–363
- Goyer A, Johnson TL, Olsen LJ, Collakova E, Shachar-Hill Y, Rhodes D, Hanson AD (2004) Characterization and metabolic function of a peroxisomal sarcosine and pipecolate oxidase from *Arabidopsis*. *J Biol Chem* 279:16947–16953
- Guo K, Ma X, Sun G, Zhao Y, Li X, Zhao W, Kai L (2006) Expression and characterization of a thermostable sarcosine oxidase (SOX) from *Bacillus* sp. in *Escherichia coli*. *Appl Microbiol Biot* 73:559–566
- Hames BD (1998) Gel electrophoresis of protein. Oxford University Press, New York
- Hassan-Abdallah A, Zhao G, Eschenbrenner M, Chen ZW, Mathews FS, Jorns MS (2005) Cloning, expression and crystallization of heterotetrameric sarcosine oxidase from *Pseudomonas maltophilia*. *Protein Express Purif* 43:33–43
- Hegerl R (1996) The EM program package: a platform for image processing in biological electron microscopy. *J Struct Biol* 116:30–34
- Kawakami R, Sakuraba H, Ohshima T (2004) Gene and primary structures of dye-linked L-proline dehydrogenase from the hyperthermophilic archaeon *Thermococcus profundus* show the presence of a novel heterotetrameric amino acid dehydrogenase complex. *Extremophiles* 8:99–108
- Kawakami R, Sakuraba H, Tsuge H, Goda S, Katunuma N, Ohshima T (2005) A second novel dye-linked L-proline dehydrogenase complex is present in the hyperthermophilic archaeon *Pyrococcus horikoshii* OT-3. *FEBS J* 272:4044–4054
- Kim JM, Shimizu S, Yamada H (1987) Crystallization and characterization of sarcosine oxidase from *Alcaligenes denitrificans* subsp. *Agr Biol Chem* 51:1167–1168
- Marco S, Urena D, Carrascosa JL, Waldmann T, Peters J, Hegerl R, Pfeifer G, Sack-Kongehl H, Baumeister W (1994) The molecular chaperone TF55: segment of symmetry. *FEBS Lett* 341:152–155
- Meškys R, Rudomanskis R, Leipuvienė R (1996) Cloning of genes encoding heterotetrameric sarcosine oxidase from *Arthrobacter* sp. *Biotechnol Lett* 18:781–786
- Nagata K, Sasaki H, Ohtsuka J, Hua M, Okai M, Kubota K, Kamo M, Ito K, Ichikawa T, Koyama Y, Tanokura M (2005) Crystal structure of monomeric sarcosine oxidase from *Bacillus* sp. NS-129 reveals multiple conformations at the active-site loop. *Proc Jpn Acad Ser B* 81:220–224
- Nishiya Y, Imanaka T (1993) Cloning and sequencing of the sarcosine oxidase gene from *Arthrobacter* sp. TE 1826. *J Ferment Bioeng* 75:239–244
- Sakuraba H, Takamatsu Y, Satomura T, Kawakami R, Ohshima T (2001) Purification, characterization, and application of a novel dye-linked L-proline dehydrogenase from a hyperthermophilic archaeon, *Thermococcus profundus*. *Appl Environ Microbiol* 67:1470–1475
- Saxton WO, Pitt TJ, Horner M (1979) Digital image processing: the Semper system. *Ultramicroscopy* 4:343–353
- Suzuki M (1981) Purification and some properties of sarcosine oxidase from *Corynebacterium* sp. U-96. *J Biochem* 89:599–607
- Suzuki H (1994) Sarcosine oxidase: structure, function, and the application to creatinine determination. *Amino Acids* 7:27–43
- Tsuge H, Kawakami R, Sakuraba H, Ago H, Miyano M, Aki K, Katunuma N, Ohshima T (2005) Crystal structure of a novel FAD-, FMN-, and ATP-containing L-proline dehydrogenase complex from *Pyrococcus horikoshii*. *J Biol Chem* 280:31045–31049
- van Heel M, Frank J (1981) Use of multivariate statistics in analysing the images of biological macromolecules. *Ultramicroscopy* 6:187–194
- Wagner MA, Schuman Jorns M (1997) Folate utilization by monomeric versus heterotetrameric sarcosine oxidases. *Arch Biochem Biophys* 342:176–181
- Willie A, Jorns M (1995) Discovery of a third coenzyme in sarcosine oxidase. *Biochemistry* 34:16703–16707